# Position–theta-phase model of hippocampal place cell activity applied to quantification of running speed modulation of firing rate

Kathryn McClain[a,b,1], David Tingley[b], David J. Heeger[a,c,1], and György Buzsáki[a,b,1]

[a]Center for Neural Science, New York University, New York, NY 10003; [b]Neuroscience Institute, New York University, New York, NY 10016; and [c]Department of Psychology, New York University, New York, NY 10003

Edited by Terrence J. Sejnowski, Salk Institute for Biological Studies, La Jolla, CA, and approved November 18, 2019 (received for review July 24, 2019)

**Spiking activity of place cells in the hippocampus encodes the animal's position as it moves through an environment. Within a cell's place field, both the firing rate and the phase of spiking in the local theta oscillation contain spatial information. We propose a position–theta-phase (PTP) model that captures the simultaneous expression of the firing-rate code and theta-phase code in place cell spiking. This model parametrically characterizes place fields to compare across cells, time, and conditions; generates realistic place cell simulation data; and conceptualizes a framework for principled hypothesis testing to identify additional features of place cell activity. We use the PTP model to assess the effect of running speed in place cell data recorded from rats running on linear tracks. For the majority of place fields, we do not find evidence for speed modulation of the firing rate. For a small subset of place fields, we find firing rates significantly increase or decrease with speed. We use the PTP model to compare candidate mechanisms of speed modulation in significantly modulated fields and determine that speed acts as a gain control on the magnitude of firing rate. Our model provides a tool that connects rigorous analysis with a computational framework for understanding place cell activity.**

spatial navigation | phase precession | firing rate variability

Place cells in the rodent hippocampus encode spatial information through their spiking activity. As the rodent moves through an environment, the firing rate of place cells increases at particular locations, termed "place fields," suggesting a firing rate code for position (1). Meanwhile, the local field potential in the hippocampus is dominated by a 7- to 9-Hz "theta" oscillation, and place cell spiking is modulated according to the phase of this oscillation (2). The phase at which spiking occurs precesses as the animal moves through the place field, a phenomena known as "phase precession" (2). Two overlapping codes for position emerge: a rate code and a phase code.

It has been suggested that the phase code is used to identify the animal's location, while the firing rate can be used to encode other variables, such as the speed of the animal's movement (3). Indeed, firing rate variability from trial to trial has been a long-noted and unexplained feature of place cell activity (4–6). In support of this hypothesis, several papers have reported a positive correlation between running speed and firing rate of pyramidal neurons in the hippocampus (7–9), entorhinal cortex (10–13), and neocortical neurons (14, 15). Replicability of this effect in hippocampus has only recently been questioned (16).

Analyzing the influence of additional variables (such as running speed) on place cell firing is difficult for several practical reasons. First, the experimenter has only limited control over the relevant variables (position, running speed, theta phase), making the behavioral paradigm nearly impossible to design without introducing additional interfering elements. Second, rodents will only run a small number of trials on a given day, typically dozens, giving us limited statistical power for analyzing effects across multiple dimensions.

Another challenge in understanding this system is the dynamic interaction between the rate code and phase code. As these codes combine, different formats of information are conveyed simultaneously in place cell spiking. The interaction can produce unintuitive, although entirely predictable, results in traditional analyses of place cell activity. These practical challenges have hindered the effort to explain variability in hippocampal firing rates. A computational tool is needed that accounts for the well-established features of this system and provides a path forward in asking further questions.

We have drawn from classic generalized linear model (13, 17), gain control models (18–20), and phase-precession models (21, 22) to develop a position–theta-phase (PTP) model of place cell activity. In this model, spatial input is scaled by theta-phase modulation to determine the firing rate of a place cell. This model has 3 primary utilities:

1) It provides a quantitative description of the relevant features of place cell activity. The model can be reliably fit with fewer than 100 spikes. These descriptive statistics can be compared across time, conditions, and cells.

## Significance

**The hippocampus is heavily studied in the context of spatial navigation, and the format of spatial information in the hippocampus is multifaceted and complex. Furthermore, the hippocampus is also thought to contain information about other important aspects of behavior such as running speed, although there is not agreement on the nature and magnitude of their effect. To understand how all of these variables are simultaneously represented and used to guide behavior, a theoretical framework is needed that can be directly applied to the data we record. We present a model that captures well-established spatial-encoding features of hippocampal activity and provides the opportunity to identify and incorporate novel features for our collective understanding.**

Author contributions: K.M., D.J.H., and G.B. designed research; K.M. and D.T. performed research; K.M. analyzed data; and K.M., D.J.H., and G.B. wrote the paper.

The authors declare no competing interest.

This article is a PNAS Direct Submission.



Data deposition: The code, demonstrations, and example data for the PTP model reported in this paper have been deposited at https://github.com/kmcclain001/ptpModel. The raw data reported in this paper have been deposited at https://buzsakilab.com/wp/datasets/. Preprocessing scripts as well as a list of experimental sessions used in this study have been deposited at https://github.com/kmcclain001/dataProcessing.

[1]To whom correspondence may be addressed. Email: km3911@nyu.edu, david.heeger@nyu.edu, or gyorgy.buzsaki@nyulangone.org.

This article contains supporting information online at https://www.pnas.org/lookup/suppl/doi:10.1073/pnas.1912792116/-/DCSupplemental.

First published December 16, 2019.

2) The model can easily generate simulated place cell data that mimic real place cell activity. The simulated data can be used for analysis on its own, or as statistical grounding in analyses of real data.
3) It introduces a framework for principled hypothesis testing. By iteratively adjusting features of the model and using a model fit comparison with the proposed baseline model, we can assess the influence of additional modulating variables.

We demonstrate these utilities and use the model to assess speed modulation in place cells. We find no evidence for speed modulation in the majority of place fields. For a minority of place fields, spiking is either positively or negatively modulated by speed. The modulation appears to act as a gain control on the overall magnitude of firing, as opposed to other candidate computations. Our PTP model offers a disciplined tool to separate physiological mechanisms from spurious statistical artifacts that may result from nonintuitive interactions of observed variables.

## Results

**Parametric Model of Place Cell Activity.** We model place cell activity as a function of 2 independent inputs: position and theta phase (Fig. 1*A*). Place cell activity is canonically described as a Gaussian function of position over a discrete portion of the environment. These portions ("place fields") are analogous to sensory receptive fields for place cells. Place cell spiking outside of the place field is typically sparse and has not been characterized; therefore, our model focuses on within-place field spiking. The spatially activated responses are modulated according to the phase of the theta oscillation, and the preferred phase of the modulation changes with position, precessing to earlier phases of the theta cycle as the animal moves through the field (2, 22, 23). This endows the phase of each spike with spatial information, along with the magnitude of the firing rate. We formalized these concepts by modeling firing rate as a Gaussian spatial response function, scaled by a Von Mises theta modulation function (Fig. 1*B*). The preferred phase of the theta modulation function shifts with position according to the linear precession function. We modeled spiking as an inhomogeneous Poisson process of the firing rate.

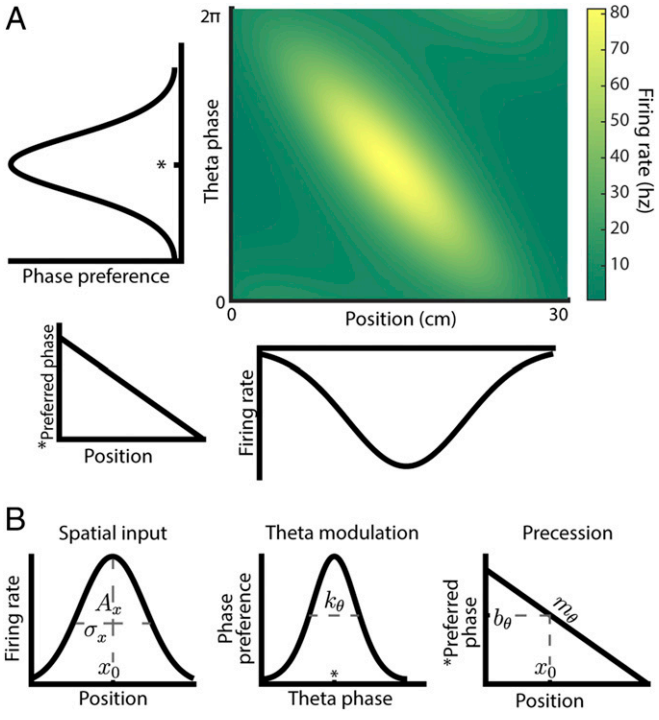


**Fig. 1.** Parametric model of place cell activity. (*A*) Schematic of model: firing rate at each theta phase and position predicted by the PTP model (heatmap). The firing rates are derived by multiplying the spatial tuning curve (below *x* axis) with the theta-phase tuning curve (beside *y* axis). The theta-phase tuning curve shifts as the preferred phase (*) decreases as a function of position (*Lower Left*), capturing phase precession. Parameters for this schematic derived from fitting model to real place field data. (*B*) Model equations: Spatial input function is a Gaussian function of position with 3 parameters: amplitude $A_x$, width $\sigma_x$, and center $x_0$. Theta modulation function is a Von Mises function (approximately circular Gaussian) of theta phase normalized to height 1 with one parameter: $k_\theta$. Theta modulation is centered on a preferred phase in the precession function, which changes linearly with position according to slope $m_\theta$ and intercept $b_\theta$.

The PTP model functions are determined by parameters that correspond to relevant functional features of place cell activity (Fig. 1*B*). The amplitude of the firing rate is parameterized by $A_x$. The width and position of the place field are captured by $\sigma_x$ and $x_0$, respectively. The theta-phase selectivity is determined by $k_\theta$. Cells that spike within a narrow range of phases have high selectivity, while cells that spike across the whole cycle have low selectivity. $m_\theta$ determines the rate of phase precession, and the preferred phase at the center of the place field is $b_\theta$.

**Fitting and Simulating Place Cell Activity.** We fit the model to spiking data recorded from place cells in rats. We examined data recorded from dorsal CA1 region of the hippocampus in rats as they ran along linear tracks (24). We used the rat's position, theta phase, and spike timing to estimate parameter values for each place field (*Methods* and *SI Appendix*, Fig. S1). Parameter values were stable across random subsets of data (*SI Appendix*, Fig. S2), indicating that our fitting procedure is reliable for this quantity of experimental data. With the parameter estimates for individual place fields as well as the distribution of parameters across the whole population, we were able to generate empirically grounded simulation data.

Using parameters estimated from an example place field, we generated place cell spiking in a simulated experiment (Fig. 2). For each simulated trial, a virtual rat ran through the place field at a constant speed while theta oscillated at a constant frequency, resulting in a straight trajectory through phase–position space (Fig. 2*A*, *i*). The PTP model predicted the firing rate at each point along this trajectory and simulated spiking as a stochastic Poisson process of the instantaneous firing rate (Fig. 2*A*, *ii*). From one trial to the next, the initial theta phase at the beginning of the field randomly shifted, as it does in real experiments (*SI Appendix*, Fig. S3), which resulted in spatially shifted firing rate patterns. Note the distinction between the initial theta phase at the entrance to the place field that we refer to here, i.e., oscillation phase that happens to occur at that particular time and location, and the onset phase of precession.

The magnitude of firing rates predicted by the PTP model is larger than typically reported for place cells. The range of firing rates for place cells within their place field has been reported as 1 to 40 Hz based on the trial-averaged firing rate within the place field (3, 25). However, on individual trials, our model predicts 80- to 100-Hz peak firing rate for many cells (Fig. 2*A*, *ii*, and *SI Appendix*, Fig. S4). The discrepancy arises from trial averaging, which averages out the effect of the theta modulation, resulting in an averaged peak firing rate roughly one-half the true peak firing rate (Fig. 2*B*, *i*).

Intertrial randomness in the theta phase at the beginning of the place field could also explain part of the variability in place cell firing rates. We simulated 2 trials with the same parameters and running speed, varying only the initial theta phase at the entry to the place field (Fig. 3*A*). The theta modulation was

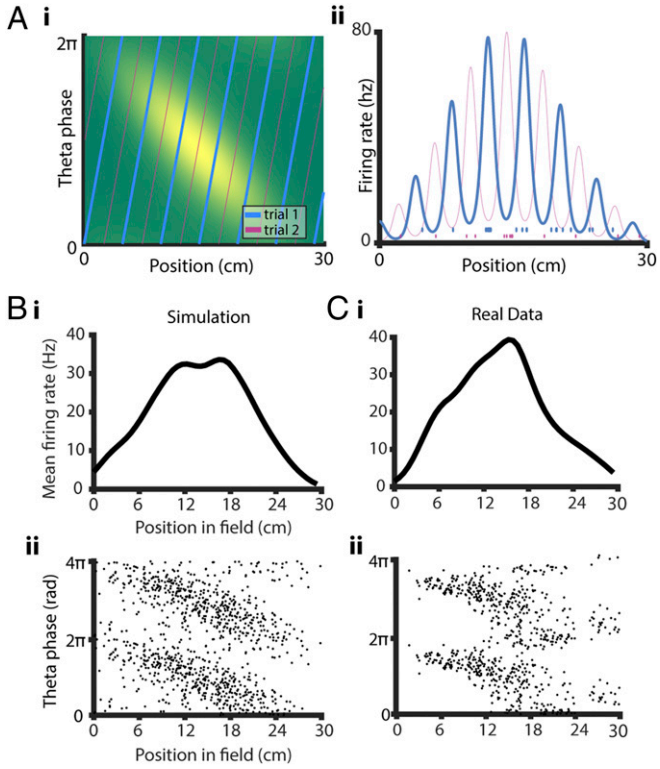


**Fig. 2.** Simulating place cell data. (*A*) Single-trial simulation. (*i*) Simulated theta-phase–position trajectory imposed on place field schematic (as in Fig. 1*A*) for trial 1 (blue), and trial 2 (purple) at the same speed with a different initial theta phase at the start of the place field [not to be confused with onset of phase precession, i.e., the preferred phase at position 0 (2)]. (*ii*) Simulated firing rates for model fit to place field in *C* computed for trajectories in trial 1 and 2 in *i*. Spiking for each trial (below) simulated via Poisson process. (*B*) Summary visualization of simulated data: Spiking was simulated for 42 trials with varying speeds and initial theta phases, using the best-fit PTP model from real place cell in *C*. (*i*) Mean firing rate vs. position, averaged over trials. (*ii*) Theta phase vs. position for each spike. (*C*) Summary visualization of real place cell data in example place field. (*i* and *ii*) Same as in *B*.

shifted with respect to the spatial input, which changed the predicted firing rate across the field by a factor of 2. Including the Poisson variability of spiking, the firing rate within the field could reasonably be 4 Hz on trial 1 and 16 Hz on trial 2. This difference is based solely on the initial theta phase and Poisson variability (6).*

The effect of the initial theta phase on firing rate is amplified at faster running speeds. We used the PTP model to predict the firing rate as a function of both running speed and initial theta phase (Fig. 3*B*). At slow speeds, the initial theta phase is not very influential in the overall rate; however, at fast speeds, the expected rate can vary dramatically. The intuition behind this observation is when the animal runs slowly, many theta cycles occur within the place field, making the alignment of any particular cycle less important for the overall predicted firing rate. At faster speeds, there are fewer cycles, making the coincidence of the theta modulation and spatial input much more important.

*Differences between phase precession in single trials vs. data pooled across trials have been reported previously (6). However, we find that the PTP model replicates this result (*SI Appendix*, Fig. S5), demonstrating that it is a natural consequence of the simple assumptions of this model. We hypothesize that the difference in sample size between pooled and single-trial data, as well as the method used to compute circular correlations may be the primary cause of this effect.

The speed-dependent variability could produce spurious correlations between speed and firing rate. We simulated a place cell experiment 3 times with identical conditions (Fig. 3*C*). In each experiment, we randomly varied running speed and initial theta phase, drawing from a uniform distribution of each, and used the model to generate spikes. We computed the average firing rate at each position for the fast, medium, and slow trials. Across the 3 simulations, an apparently negative relationship between speed and firing rate arose in one, no relationship was evident in another, and a positive relationship appeared in the last. Recall the model used for simulation has no explicit speed dependence, so each of the apparent relationships is artifactual. The confound between running speed and firing-rate variability makes the analysis of speed tuning in place cells difficult, because standard statistics are not sufficient to assess the significance of these relationships.

**Quantifying the Effect of Running Speed on Place Cell Activity.** In real place field data, we found a heterogeneous distribution of speed dependence using standard correlations. We computed the average speed and firing rate within the place field for each trial and calculated the correlation across trials. Contrary to previous findings that have reported mostly positive correlations between running speed and firing rate (3, 7), and in line with a more recent report (16), we found place fields with ostensible negative speed

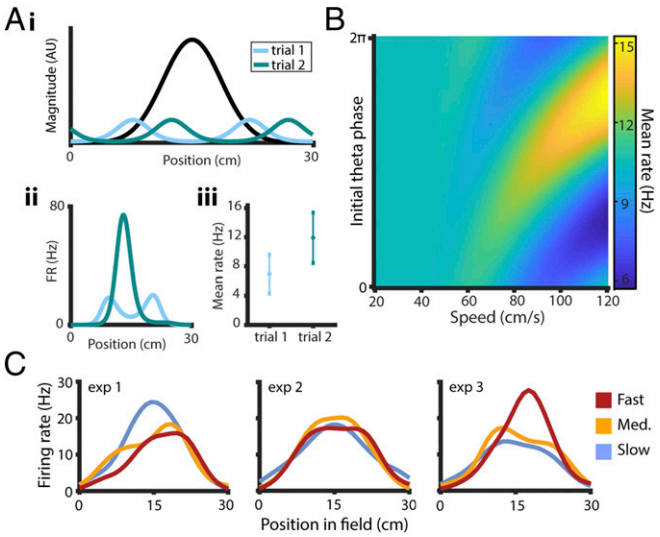


**Fig. 3.** Speed-dependent variability can cause spurious correlations with running speed. (*A*) Alignment between spatial input and theta modulation can affect expected firing rate in place fields. Position and theta phase are simulated for 2 trials with identical running speed, differing only in the initial theta phase at the entrance of the place field. The resulting model equations and predicted firing rates are shown: (*i*) The spatial input function (black) is identical for the 2 trials, while the phase modulation functions are shifted according to the initial theta phase for trials 1 (blue) and 2 (green). (*ii*) Predicted firing rate vs. position for trials 1 and 2 computed by multiplying the spatial input and phase modulation functions in *i*. (*iii*) Mean firing rates for trials 1 and 2, averaged over position. Error bars correspond to SE (SEM) predicted from Poisson variance of spiking. (*B*) Mean firing rate across place field simulated as a function of initial theta phase and running speed. Variability caused by initial theta phase increases at higher speeds. (*C*) Firing rate vs. position in the fast (red), medium (yellow), and slow (blue) sets of trials in 3 simulated experiments. In each experiment, 30 trials were simulated with randomized speeds and initial theta phases. Mean firing rate was computed as a function of position for each set of trials. Conditions were identical for each simulated experiment with no explicit speed dependence in the model; however, apparent speed modulation appeared by chance, both negatively (experiment 1) and positively (experiment 3).

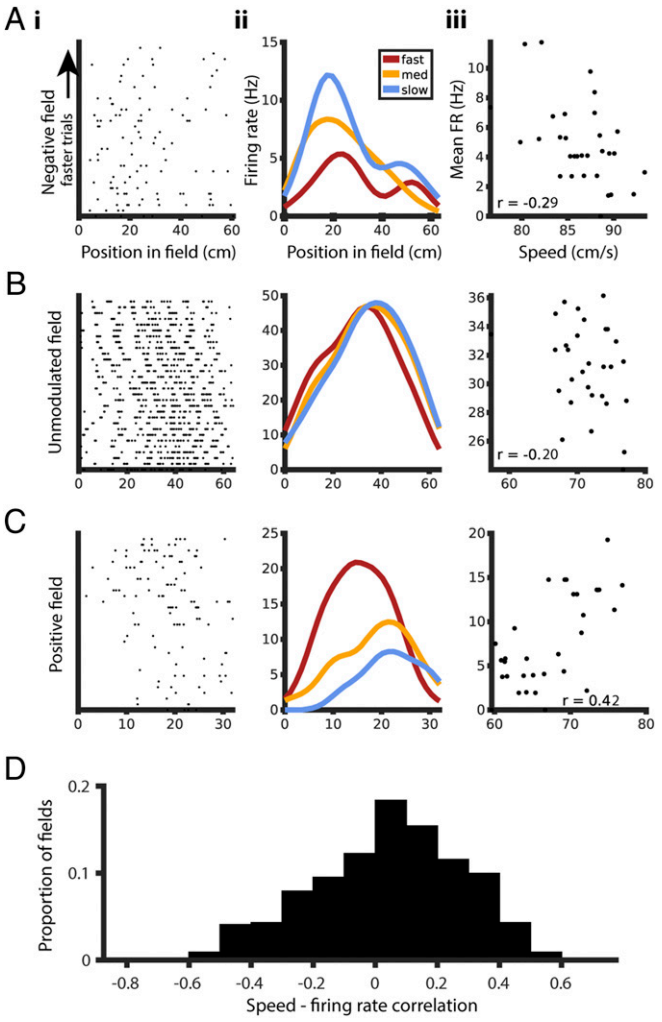


**Fig. 4.** Real pyramidal cells show heterogeneous distribution of speed correlations. (*A*) Speed dependence of example place field with ostensible negative speed modulation: (*i*) Trial vs. position of each spike, trials ordered by mean running speed in the place field. (*ii*) Firing rate vs. position for fastest (red), middle (yellow), and slowest (blue) thirds of trials. (*iii*) Mean firing rate across place field vs. speed, each point representing one trial. *r* values throughout indicate Kendall rank correlation coefficient ($P = 0.025$). (*B*) Same as *A* for ostensibly unmodulated example place field ($P = 0.13$). (*C*) Same as *A* for ostensibly positively speed-modulated place field ($P = 8.8e\text{-}04$). (*D*) Distribution of speed–firing-rate correlations across all place fields in dataset.

relationships (Fig. 4*A*) as well as those with apparently positive relationships (Fig. 4*C*). We also found a majority of place fields that did not appear to be speed modulated (Fig. 4*B*). Across all place fields in the dataset, the distribution of correlations appeared to be heterogeneous (Fig. 4*D*). However, because speed-related variability can produce spurious correlations (Fig. 3*C*), these apparent effects must be scrutinized.

To more rigorously assess speed modulation, we used the PTP model to generate an ensemble of simulated experiments, from which we computed a null distribution of speed correlations. We use "null distribution" because the PTP model has no speed dependence, so the resulting correlations arise solely from the sources of variability accounted for in this model. For each place field in our dataset, we used the estimated model parameters to virtually recreate the experiment (Fig. 5*A*). We computed the correlation between speed and simulated firing rate, and then repeated the simulated experiments 20,000 times to compute a null distribution of correlation values (Fig. 5*B*). The null distribution varies across place fields depending on the best-fit model parameters for each individual field, and so must be computed independently.

Speed–firing-rate correlations for most place fields did not lie significantly outside the respective null distributions. The distance between the true correlation value and the null distribution was measured as a *P* value in the positive and negative directions (Fig. 5*C*). A criterion of $P < 0.05$ was used, and fields with significant positive and negative modulation were identified. A subset of place fields with positive modulation (19%) and a subset with negative modulation (12%) were identified above chance levels. Nonetheless, the majority of place fields (69%) did not meet our criterion for significant speed modulation (Fig. 5*D*). In summary, we found that the degree of speed modulation in the majority of place fields lies within the predictions of the PTP model, which does not include any speed dependence. However, we found a minority of place fields with speed modulation beyond the model predictions. Next, we sought the potential mechanisms of such effects.

We extended the PTP model to explore the computational effect of speed on firing rates of significantly modulated place fields. The model delineates the independent features of place fields that could be affected by running speed. Two candidates that could

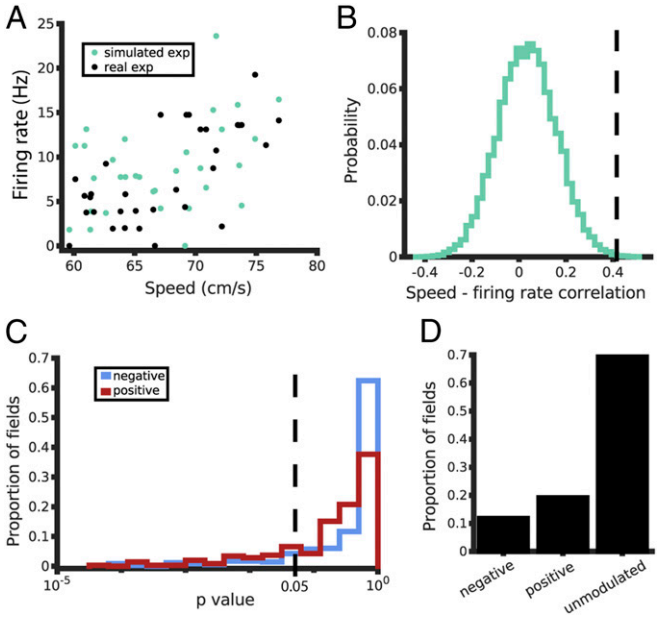


**Fig. 5.** Speed modulation is statistically significant in a small number of place fields. (*A*) Mean firing rate vs. speed for real example place field (same as Fig. 4*C*), for real experiment (black) and simulated experiment (green). Simulation performed using model fit to this place field and conditions identical to real experiment. Kendall correlation coefficient for simulated experiment is $r = 0.27$ ($P = 0.032$). (*B*) Null distribution of speed–firing-rate correlations (green) computed from 20,000 simulations of the experiment in *A*, each using the empirically measured position and theta phase from the original experiment. Empirical correlation in black. For this example field, we find evidence for speed modulation beyond what can be explained by the PTP model ($P = 0.001$). (*C*) One-tailed *P* values computed from null distribution for all place fields in the dataset. Two tests are shown, one for positive speed–firing-rate relationships (red) and one for negative speed–firing-rate relationships (blue). Values range from 0 to 1, corresponding to the proportion of simulated experiments with correlation values larger (for negative test) or smaller (for positive test) than that of the real experiment. Significant speed modulation is defined as $P < 0.05$. (*D*) Proportion of place fields for which there was statistical significance for negative or positive speed modulation, and the proportion for which there was no evidence for speed modulation.

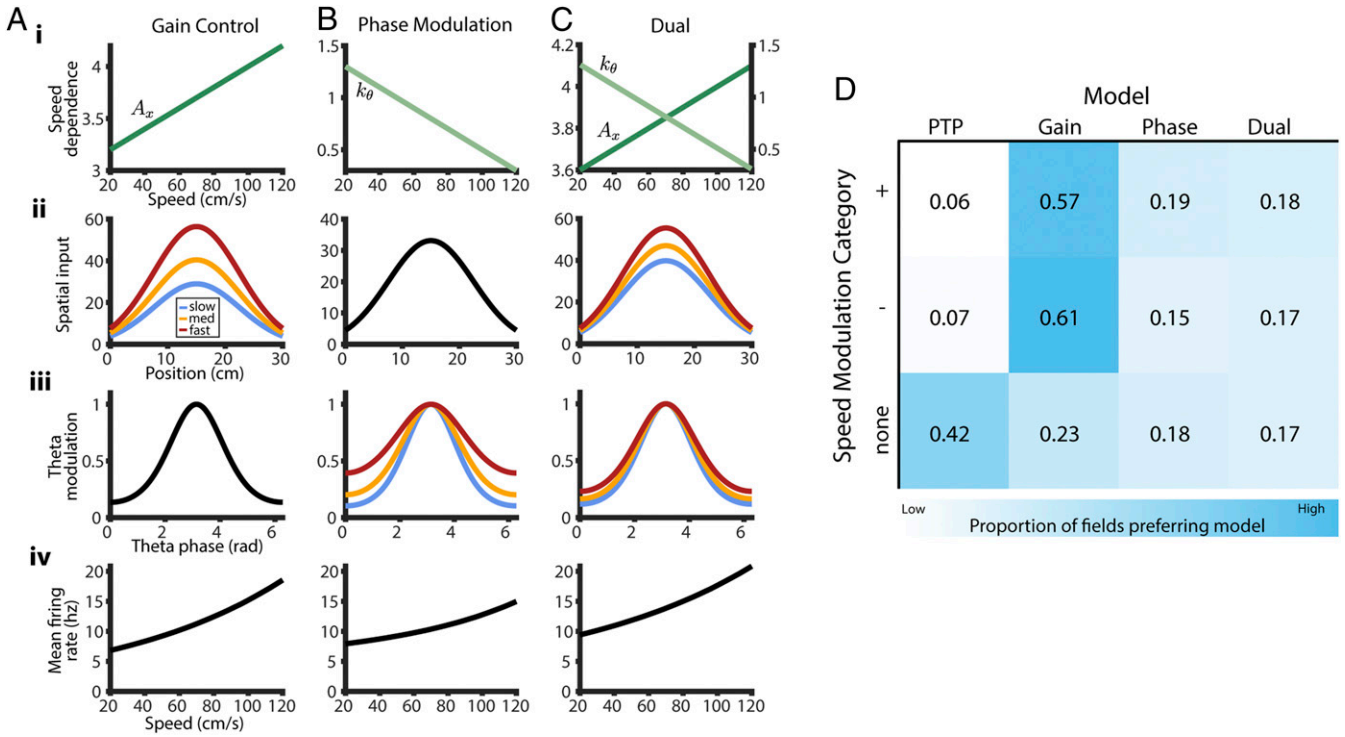


**Fig. 6.** Speed model comparison: variants of basic model that include speed dependence. (*A*) Gain control model: (*i*) Hypothetical relationship between amplitude parameter and speed. (*ii*) Spatial input function as it varies with speed. (*iii*) Phase modulation function (stationary with respect to speed). (*iv*) Hypothetical relationship between firing rate and speed for gain control model. (*B*) Phase modulation model: same as *A*, except phase selectivity varies with speed instead of amplitude. (*C*) Dual modulation model: same as *A*, except both amplitude and phase selectivity vary with speed. (*D*) Proportion of place fields in each speed modulation category best fit by each model variant. Positively and negatively modulated fields are by majority best fit with a gain control model, while unmodulated fields are mostly best fit with the original PTP model.

directly impact the average firing rate in the place field are the amplitude $A_x$ (Fig. 6*A*) and the phase selectivity $k_\theta$ (Fig. 6*B*).† Modeling amplitude as a function of speed corresponds to a gain control model, where running speed multiplicatively scales the magnitude of activity. Modeling phase selectivity as a function of speed corresponds to a changing window of spiking within the theta cycle. These 2 mechanisms could also work in consort in a dual-speed model (Fig. 6*C*). In each of these speed-dependent variants of our original model, we model the speed-dependent parameter as a linear function of speed. The slope of this function determines the direction and degree of speed dependence (23).

Significantly speed-modulated place fields are best explained by a gain control model of speed. We performed a model fit comparison for each place field, comparing the speed-dependent model variants and the original place field model. For each place field, we fit each model and measured the performance of the model in predicting a held-out subset of the data. We selected the model with the highest average log-likelihood as the preferred model for that place field (*Methods*). Expectedly, the majority of unmodulated place fields preferred the original PTP model (Fig. 6*D*). Among the subsets of positively and negatively modulated place fields, the majority preferred a gain control model of speed modulation. These results suggest the computational effect of speed operates primarily on the magnitude of place cell activity, leaving the theta-phase modulation of place cells unaffected.

## Discussion

**Refining Previous Notions of Speed Modulation of Firing Rates.** Our analysis of speed modulation in place cell activity provides some amendments to previous notions in the spatial navigation field. We did not find evidence for speed modulation in the majority of place cells and suggest increased firing rate variability at high speeds as a potential source of spurious correlations. Of the minority of fields that did show modulation, some were positively modulated and others were negatively modulated. For each of these subsets, speed appears to affect the activity primarily as a gain control, scaling the overall magnitude, while theta modulation remains mostly unaffected (8, 21, 26–28).‡

The lack of robust speed dependence of place cell firing rates may convey an important robustness of the system. If place cells are used to for navigation purposes, altering the "code" for behavioral parameters such as running speed may not be advantageous. Interleaving codes through gain control computations can allow one population to simultaneously represent multiple variables (3, 19, 29–31), and our results do suggest that speed dependence in a minority of place fields is best characterized as gain control. However, the sparsity of place cells in our data showing any speed dependence makes this interpretation tenuous.

An additional consideration in studying "speed modulation" is the relationship between speed and trial number that exists in almost all experiments. As the animal's motivation decreases throughout the course of an experiment, running speed also

†Other features of a place field could also be affected by speed, such as the properties of phase precession (23). However, our model does not predict that speed dependence of phase precession will have an effect on firing rate (*SI Appendix*, Fig. S6).

‡A positive relationship between theta frequency and running speed has been reported in many studies (21, 26, 27) and questioned by others (8, 28). Through simulation, we find that, regardless of the relationship, changing theta frequency does not affect estimated firing rate across the place field (*SI Appendix*, Fig. S7).

decreases, causing an inseparable correlation between speed and trial number (*SI Appendix*, Fig. S8). This may be a confounding variable as neural signals associated with velocity are reciprocally woven into neural circuits that control motivated behavior (32–34). What has been identified as "speed modulation" in this report, and likely in others, could also be considered a motivation signal modulating activity, or simply "drift," i.e., slow changes in activity patterns over time. In terms of functionally characterizing sources of variability in the system, such a distinction may not be important, because speed, time, and motivation are correlated. However, if the goal is to identify underlying physiological mechanisms of the effect, it should become an important consideration.

A quantitative characterization of drift over time in place field activity is a much-needed analysis for hippocampal research that our PTP model would be suited to address. As experimenters probe physiological circuits by performing manipulations and recording multiple changes, a baseline characterization of the volatility is needed to specify the effects caused by the manipulations and separate them from appealing, although ultimately spurious effects.

Our findings do not contradict suggestions that speed is a fundamental parameter of hippocampal activity. We found that the firing rates of the majority of putative fast-spiking interneurons, but not those of slow-spiking interneurons, were positively modulated by running speed (*SI Appendix*, Fig. S9). Fast-spiking interneurons, rather than pyramidal cells or slow-spiking interneurons, may be responsible for speed control of frequency of theta oscillation of hippocampal place cells (2, 21, 35, 36) and entorhinal grid cells (37).

**The PTP Model: Uses and Findings.** The PTP model we describe here provides a functional description of the well-established factors that influence place cell activity: position and theta phase. Position is an external variable that exists in space, while the theta oscillation is entirely internally generated and propagates in time. These variables interact dynamically through running speed, which may exert its own place field-specific influence on activity. The results of this interaction are not always obvious or intuitive. Our model can be used in lieu of intuition to inform baseline controls. Appropriate controls are necessary to ward against interpreting inherent implications of the position–phase interaction as novel features of place cell activity. Our model also provides a framework for identifying and incorporating truly novel features into our collective understanding of hippocampal operations.

The PTP model has allowed us to uncover a few surprising features of place cell activity. First, the dynamic range of place cell firing rate is roughly double what is typically measured from trial-averaged firing rates. Second, running speed affects firing rate variability due to Poisson randomness and alignment between theta phase and position, which can produce spurious correlations between speed and firing rate. Finally, despite the potential for spurious correlations, there appear to be small subsets of place fields that show genuine speed modulation.

In general, the PTP model can be used in several ways. First, key features of place fields can be described quantitatively by fitting the model with relatively small amounts of place cell data. Second, realistic place cell data can be generated in simulated experiments, with conditions and parameters fully controlled by the experimenter. Simulated place cell data can help explore theoretical aspects of the hippocampal spatial navigation system, inform the design of future experiments, and serve as a control in analyzing real place cell data. Last, hypothetical variations of the model can be systematically tested to uncover additional features of the data as demonstrated in Fig. 6.

**Model Limitations and Extensions.** In formulating our model, choices were made for the sake of simplicity that may have neglected some particular specifics of hippocampal physiology. For example, formulating phase precession as a linear function of position (2, 3) ignores previous work that has characterized a curved "banana"-shaped phase precession (25, 38). Skewness of place fields, which may emerge with experience (39), is another interesting feature that is not captured by the symmetric spatial input function of our model. However, the PTP model can be amended to accommodate details of such properties, and be a useful tool for further probing their significance.

Physical stationarity of the place field is a more fundamental assumption of the PTP model. We define the spatial input function as an environmental input drive at a particular location (1). An alternate interpretation is that a place field begins at the occurrence of the first spike, and the place field peak varies from trial to trial (5, 6), tying the place field more strongly to theta phase than to position. This interpretation may be useful in some contexts, but ours reflects common assumptions in the field that are arguably more relevant in the context of spatial navigation.

One-dimensional space is another assumption. In its current instantiation, the PTP model is not directly applicable for 2D navigation. It is possible to expand the model to 2 dimensions; however, the exact form of this expansion raises interesting theoretical and experimental questions about phase precession in multiple dimensions. Two opposing hypotheses could include the following: 1) preferred phase is tied to allocentric space, meaning the phase precession function would change depending on the direction of travel; or 2) phase precession is constant, meaning the preferred phase at one location would be drastically different depending on the direction of travel, suggesting theta phase is an egocentric code (25, 40, 41). These 2 hypotheses could be compared in real data using variations of the PTP model, and their implications for spatial navigation could be explored.

We also use a Poisson noise model to capture stochasticity of place cell spiking. We capture theta-time-scale fluctuations in the underlying rate. Pyramidal cells in hippocampus reportedly spike in bursts (42), which may be explained by an underlying mechanism faster than the theta modulation. It is possible that true spiking statistics could be more accurately replicated with the addition of faster variables or history dependence. The PTP model could serve as an effective null model to test for the role and effects of faster spiking properties in place cells.

We also only model single place fields, while real place cells can have multiple fields within an environment (43, 44). As is, PTP models for multiple fields could easily be combined along an expanded position axis. A potentially interesting extension could involve using optimization to automatically identify place fields and model them jointly.

The PTP model describes the interaction between position and theta phase as the primary factors that affect place cell activity. The interaction of these variables is specific to place cells, yet multiple variables might have similarly specific interactions that affect firing rates in other functions and regions of the spatial navigation system (35, 45–47). We hope our general statistical approach can be used to promote rigor in the study of spatial navigation and connect analyses to broader computational frameworks.

## Methods

**Parametric Model of Place Cell Activity.** The model is defined by 3 equations, where $x$ is the position within the field and $\theta$ is the phase of the theta oscillation:

Spatial input equation:

$$f(x) = \exp(A_x) \cdot \exp\left(\frac{-(x - x_0)^2}{2\sigma_x^2}\right);$$

Phase modulation equation:

$$g(\theta, x) = \exp(k_\theta \cdot (\cos(\theta - \theta_0(x)) - 1));$$

Phase precession equation:

$$\theta_0(x) = b_\theta + m_\theta(x - x_0).$$

The rate is modeled as a product of the spatial input and phase modulation equations:

$$r(x, \theta) = f(x) \cdot g(\theta, x).$$

Intuitively, $f$ can be considered a firing rate, with units of hertz. $g$ is a unitless modulation of $f$. $\theta_0$, measured in radians, is the preferred theta phase of $g$, at position $x$. The position variable $x$, and parameters $x_0$ and $\sigma_x$, are measured in arbitrary units normalized across each place field, but can easily be converted to cm by multiplying by the measured width of the field, as we do throughout this report for ease of visualization.

The number of spikes $k_t$ occurring at position $x_t$ and theta phase $\theta_t$ over interval $dt$ is modeled as a Poisson probability distribution with mean $\lambda_t = dt \cdot r(x_t, \theta_t)$:

$$p(k_t|\lambda_t) = \frac{\lambda_t^{k_t} e^{-\lambda_t}}{k_t!}.$$

The likelihood that a model produced the data were computed as the product of probability over time:

$$\ell = \prod_t p(k_t|\lambda_t).$$

Our model explained the spiking activity of the majority of place fields better than simpler iterations of the model (*SI Appendix*, Fig. S10). Code, demonstrations, and example data for the PTP model can be found at https://github.com/kmcclain001/ptpModel.

**Data.** Spiking and local field potential were recorded from dorsal CA1 region of the hippocampus of rats as they traversed linear tracks [as described by Tingley and Buzsáki (24)]. Datasets were curated for each place field by selecting time points while the animal was in each place field. The model was fit for each field using the data recorded at those time points. The inputs to the model consist of 4 time-series variables that are interpolated to the sampling rate of the local field potential (1,250 Hz): 1) the position of the rat within the place field, 2) phase of the theta oscillation, 3) speed of the rat within the place field (only used in explicit speed models), and 4) binary spike or no spike for each time point. The conclusions of our analyses are maintained across a reasonable range of sampling frequencies.

***Position.*** Raw position was measured as described by Tingley and Buzsáki (24). The position on the track was linearized based on the occupancy in 2D (code included). Trials were partitioned by the starting point and running direction of the rat. Place fields were defined only within trials from a single partition. Linearized position was smoothed using a Gaussian convolution kernel and interpolated cubically to 1,250 Hz. Position within each place field was normalized on a 0 to 1 scale.

***Running speed.*** Speed of the rat was computed from the raw position measurements as the Euclidean distance in 2D position between frames. Speed was smoothed with a Gaussian convolution kernel and cubically interpolated to 1,250 Hz.

***Theta phase.*** To extract the theta oscillation, the local field potential was filtered using a fourth order 4- to 15-Hz bandpass Butterworth filter. Due to speed-dependent asymmetry in the theta oscillation waveform (48), the phase within each cycle was defined by the latency between peaks in the signal and linearly interpolated from 0 to $2\pi$ between consecutive peaks.

Raw data are available at https://buzsakilab.com/wp/datasets/. Preprocessing scripts as well as a list of experimental sessions used in this study can be found at https://github.com/kmcclain001/dataProcessing.

**Model Fitting.** Models were fit to data from each place field independently. Each time point corresponded to a datapoint with a position, theta phase, running speed, and spike/no spike value. For each fit, parameters were estimated using a training dataset. A multistart fitting procedure was used with 5 randomly chosen initial points to mitigate the effects of local minima in the optimization. The fmincon function in Matlab was used to perform the optimization, constrained by reasonable parameter ranges (exact values can be found in code). If the parameter estimates did not converge 5 times, a field was discarded, which was the case for 80 fields.

**Parameter Estimation.** To assess the stability of the parameter estimates for each field, the model was fit 10 times. For each fit, 90% of the data points for that field were randomly chosen to make the training dataset (*SI Appendix*, Fig. S1). The repeated fitting provided a distribution of parameter estimates for each field (*SI Appendix*, Fig. S2). The median value for each parameter was chosen as the estimate for each field.

**Model Comparison.** To compare the performance of competing models (Fig. 6 and *SI Appendix*, Fig. S10), Monte Carlo cross-validation with averaging was used (49). Data were split 10 times, and each model was cross-validated by fitting on 75% of the data, and then testing on the remaining 25%. The mean log-likelihood for each model was computed, and the model with the highest log-likelihood was chosen. Cross-validation allowed us to make a valid comparison across models with different numbers of parameters.

**Neuron Classification.** Waveforms were clustered as described by Tingley and Buzsáki (24). Putative cell types for each cluster were identified by 4 factors: firing rate, integral of the second half of the mean waveform, and the rising slope and falling slope of the autocorrelogram fit with a double-exponential function. These 4 features were grouped using $k$-means clustering with 15 clusters. These clusters were merged manually into putative interneurons and putative pyramidal cells.

**Place Field Identification.** Place fields were identified based on the firing rate of pyramidal cells (3). The mean firing rate as a function of position was computed for each cell in each trial condition. Regions on the track where the firing rate was above 20% of the peak were isolated (44). The length of these regions had to be longer than ~1/15th the length of the track and smaller than five-eighths the length of the track. The place cell also had to spike at least once while the subject was in the field on at least four-fifths of the trials.

**ACKNOWLEDGMENTS.** We thank Cristina Savin and Daniel Levenstein for input on the development and implementation of the model, and NIH MH54671, MH107396, U19NS104590, a National Science Foundation Partnerships for International Research and Education grant, and NIH Training Grant for Computational Neuroscience T90DA043219 for funding.

1. J. O'Keefe, L. Nadel, *The Hippocampus as a Cognitive Map* (Oxford University Press, 1978).
2. J. O'Keefe, M. L. Recce, Phase relationship between hippocampal place units and the EEG theta rhythm. *Hippocampus* **3**, 317–330 (1993).
3. J. Huxter, N. Burgess, J. O'Keefe, Independent rate and temporal coding in hippocampal pyramidal cells. *Nature* **425**, 828–832 (2003).
4. A. A. Fenton, R. U. Muller, Place cell discharge is extremely variable during individual passes of the rat through the firing field. *Proc. Natl. Acad. Sci. U.S.A.* **95**, 3182–3187 (1998).
5. A. V. Olypher, P. Lánský, A. A. Fenton, Properties of the extra-positional signal in hippocampal place cell discharge derived from the overdispersion in location-specific firing. *Neuroscience* **111**, 553–566 (2002).
6. R. Schmidt *et al.*, Single-trial phase precession in the hippocampus. *J. Neurosci.* **29**, 13232–13241 (2009).
7. B. L. McNaughton, C. A. Barnes, J. O'Keefe, The contributions of position, direction, and velocity to single unit activity in the hippocampus of freely-moving rats. *Exp. Brain Res.* **52**, 41–49 (1983).
8. A. Czurkó, H. Hirase, J. Csicsvari, G. Buzsáki, Sustained activation of hippocampal pyramidal cells by "space clamping" in a running wheel. *Eur. J. Neurosci.* **11**, 344–352 (1999).
9. A. D. Ekstrom, J. Meltzer, B. L. McNaughton, C. A. Barnes, NMDA receptor antagonism blocks experience-dependent expansion of hippocampal "place fields." *Neuron* **31**, 631–638 (2001).
10. B. J. Kraus *et al.*, During running in place, grid cells integrate elapsed time and distance run. *Neuron* **88**, 578–589 (2015).
11. E. Kropff, J. E. Carmichael, M.-B. Moser, E. I. Moser, Speed cells in the medial entorhinal cortex. *Nature* **523**, 419–424 (2015).
12. J. R. Hinman, M. P. Brandon, J. R. Climer, G. W. Chapman, M. E. Hasselmo, Multiple running speed signals in medial entorhinal cortex. *Neuron* **91**, 666–679 (2016).
13. K. Hardcastle, N. Maheswaranathan, S. Ganguli, L. M. Giocomo, A multiplexed, heterogeneous, and adaptive code for navigation in medial entorhinal cortex. *Neuron* **94**, 375–387.e7 (2017).
14. Y. Fu *et al.*, A cortical circuit for gain control by behavioral state. *Cell* **156**, 1139–1152 (2014).
15. A. J. Christensen, J. W. Pillow, Running reduces firing but improves coding in rodent higher-order visual cortex. bioRxiv:10.1101/214007 (4 November 2017).
16. Z. H. T. D. Góis, A. B. L. Tort, Characterizing speed cells in the rat hippocampus. *Cell Rep.* **25**, 1872–1884.e4 (2018).
17. R. L. T. Goris, J. A. Movshon, E. P. Simoncelli, Partitioning neuronal variability. *Nat. Neurosci.* **17**, 858–865 (2014).
18. D. J. Heeger, Normalization of cell responses in cat striate cortex. *Vis. Neurosci.* **9**, 181–197 (1992).
19. J. H. Reynolds, D. J. Heeger, The normalization model of attention. *Neuron* **61**, 168–185 (2009).

20. H. R. Kim, D. E. Angelaki, G. C. DeAngelis, Gain modulation as a mechanism for coding depth from motion parallax in macaque area MT. *J. Neurosci.* **37**, 8180–8197 (2017).
21. C. Geisler, D. Robbe, M. Zugaro, A. Sirota, G. Buzsáki, Hippocampal place cell assemblies are speed-controlled oscillators. *Proc. Natl. Acad. Sci. U.S.A.* **104**, 8149–8154 (2007).
22. A. Chadwick, M. C. W. van Rossum, M. F. Nolan, Independent theta phase coding accounts for CA1 population sequences and enables flexible remapping. *eLife* **4**, e03542 (2015).
23. A. P. Maurer, S. N. Burke, P. Lipa, W. E. Skaggs, C. A. Barnes, Greater running speeds result in altered hippocampal phase sequence dynamics. *Hippocampus* **22**, 737–747 (2012).
24. D. Tingley, G. Buzsáki, Transformation of a spatial map across the hippocampal-lateral septal circuit. *Neuron* **98**, 1229–1242.e5 (2018).
25. W. E. Skaggs, B. L. McNaughton, M. A. Wilson, C. A. Barnes, Theta phase precession in hippocampal neuronal populations and the compression of temporal sequences. *Hippocampus* **6**, 149–172 (1996).
26. W. L. McFarland, H. Teitelbaum, E. K. Hedges, Relationship between hippocampal theta activity and running speed in the rat. *J. Comp. Physiol. Psychol.* **88**, 324–328 (1975).
27. S. M. Montgomery, M. I. Betancur, G. Buzsáki, Behavior-dependent coordination of multiple theta dipoles in the hippocampus. *J. Neurosci.* **29**, 1381–1394 (2009).
28. G. Chen, J. A. King, Y. Lu, F. Cacucci, N. Burgess, Spatial cell firing during virtual navigation of open arenas by head-restrained mice. *eLife* **7**, e34789 (2018).
29. A. Pouget, L. H. Snyder, Computational approaches to sensorimotor transformations. *Nat. Neurosci.* **3** (suppl.), 1192–1198 (2000).
30. A. Pouget, S. Deneve, J.-R. Duhamel, A computational perspective on the neural basis of multisensory spatial representations. *Nat. Rev. Neurosci.* **3**, 741–747 (2002).
31. J. M. Beck, P. E. Latham, A. Pouget, Marginalization in neural circuits with divisive normalization. *J. Neurosci.* **31**, 15310–15319 (2011).
32. F. Bender *et al*., Theta oscillations regulate the speed of locomotion via a hippocampus to lateral septum pathway. *Nat. Commun.* **6**, 8521 (2015).
33. F. Fuhrmann *et al*., Locomotion, theta oscillations, and the speed-correlated firing of hippocampal neurons are controlled by a medial septal glutamatergic circuit. *Neuron* **86**, 1253–1264 (2015).
34. J. Robinson *et al*., Optogenetic activation of septal glutamatergic neurons drive hippocampal theta rhythms. *J. Neurosci.* **36**, 3016–3023 (2016).
35. E. Pastalkova, V. Itskov, A. Amarasingham, G. Buzsáki, Internally generated cell assembly sequences in the rat hippocampus. *Science* **321**, 1322–1327 (2008).
36. C. Geisler *et al*., Temporal delays among place cells determine the frequency of population theta oscillations in the hippocampus. *Proc. Natl. Acad. Sci. U.S.A.* **107**, 7957–7962 (2010).
37. N. Burgess, Grid cells and theta as oscillatory interference: Theory and predictions. *Hippocampus* **18**, 1157–1174 (2008).
38. K. D. Harris *et al*., Spike train dynamics predicts theta-related phase precession in hippocampal pyramidal cells. *Nature* **417**, 738–741 (2002).
39. M. R. Mehta, C. A. Barnes, B. L. McNaughton, Experience-dependent, asymmetric expansion of hippocampal place fields. *Proc. Natl. Acad. Sci. U.S.A.* **94**, 8918–8921 (1997).
40. K. D. Harris, J. Csicsvari, H. Hirase, G. Dragoi, G. Buzsáki, Organization of cell assemblies in the hippocampus. *Nature* **424**, 552–556 (2003).
41. J. R. Huxter, T. J. Senior, K. Allen, J. Csicsvari, Theta phase-specific codes for two-dimensional position, trajectory and heading in the hippocampus. *Nat. Neurosci.* **11**, 587–594 (2008).
42. J. B. Ranck, Jr, Studies on single neurons in dorsal hippocampal formation and septum in unrestrained rats. I. Behavioral correlates and firing repertoires. *Exp. Neurol.* **41**, 461–531 (1973).
43. E. Park, D. Dvorak, A. A. Fenton, Ensemble place codes in hippocampus: CA1, CA3, and dentate gyrus place cells have multiple place fields in large environments. *PLoS One* **6**, e22349 (2011).
44. K. Mizuseki, S. Royer, K. Diba, G. Buzsáki, Activity dynamics and behavioral correlates of CA3 and CA1 hippocampal pyramidal neurons. *Hippocampus* **22**, 1659–1680 (2012).
45. M. Fyhn, S. Molden, M. P. Witter, E. I. Moser, M.-B. Moser, Spatial representation in the entorhinal cortex. *Science* **305**, 1258–1264 (2004).
46. G. Buzsáki, E. I. Moser, Memory, navigation and theta rhythm in the hippocampal-entorhinal system. *Nat. Neurosci.* **16**, 130–138 (2013).
47. H. Eichenbaum, On the integration of space, time, and memory. *Neuron* **95**, 1007–1018 (2017).
48. G. Buzsáki, P. Rappelsberger, L. Kellényi, Depth profiles of hippocampal rhythmic slow activity ("theta rhythm") depend on behaviour. *Electroencephalogr. Clin. Neurophysiol.* **61**, 77–88 (1985).
49. S. Arlot, A. Celisse, A survey of cross-validation procedures for model selection. *Stat. Surv.* **4**, 40–79 (2010).